IEEE Access
Multidisciplinary ⋮ Rapid Review ⋮ Open Access Journal

Received April 28, 2022, accepted May 31, 2022, date of publication June 10, 2022, date of current version June 20, 2022.

Digital Object Identifier 10.1109/ACCESS.2022.3181985

Deeply Trained Real-Time Body Sensor Networks for Analyzing the Symptoms of Parkinson's Disease

RAJASOUNDARAN SOUNDARARAJAN[1], A. V. PRABU[2], SIDHESWAR ROUTRAY[3], PRINCE PRIYA MALLA[4], ARUN KUMAR RAY[4], GOPINATH PALAI[5], OSAMA S. FARAGALLAH[6], MOHAMMED BAZ[7], (Senior Member, IEEE), MATOKAH M. ABUALNAJA[8], MOHAMOUD M. A. EID[9], AND AHMED NABIH ZAKI RASHED[10]

[1]School of Computing Science and Engineering, VIT University, Bhopal 466114, India
[2]Department of Electronics and Communication Engineering, Koneru Lakshmaiah Education Foundation, Guntur 522302, India
[3]Department of Computer Science and Engineering, School of Engineering, Indrashil University, Rajpur, Mehsana, Gujarat 382740, India
[4]School of Electronics Engineering, Kalinga Institute of Industrial Technology (KIIT), Bhubaneswar 751024, India
[5]Department of Electronics and Communication Engineering, Gandhi Institute for Technological Advancements, Bhubaneswar 752054, India
[6]Department of Information Technology, College of Computers and Information Technology, Taif University, Taif 21944, Saudi Arabia
[7]Department of Computer Engineering, College of Computers and Information Technology, Taif University, Taif 21944, Saudi Arabia
[8]Department of Chemistry, Faculty of Applied Science, Umm Al-Qura University, Mecca 24230, Saudi Arabia
[9]Department of Electrical Engineering, College of Engineering, Taif University, Taif 21944, Saudi Arabia
[10]Electronics and Electrical Communications Engineering Department, Faculty of Electronic Engineering, Menoufia University, Menouf 32951, Egypt

Corresponding author: Ahmed Nabih Zaki Rashed (ahmed_733@yahoo.com)

This work was supported by the Deanship of Scientific Research, Taif University Researchers Supporting Project, through Taif University, Taif, Saudi Arabia, under Grant TURSP-2020/239.

ABSTRACT Parkinson's Disease (PD) is a neural system disorder that disturbs the mental activities and physical activities of human beings. Analyzing the symptoms and biosignal data of PD is crucially focused in medical research fields. The existing PD diagnosis models are limited to real-time issues, insufficient deep data extraction, and early monitoring problems. On the scope, the proposed Optimal Health Support and PD Analysis System (OHPAS) analyses the symptoms of PD using a deeply trained biosensors network environment. The novel system trains the biosensor network using complex Machine Learning (ML) and Deep Learning (DL) approaches. The environment of OHPAS sets up acoustic sensors (UT-PF), microphones (MC-1500 unit), and multimodal sensor units (MC-10 sensor). MC-10 is the sensor suite that has an accelerometer sensor, gyro sensor, and Electro Cardio Gram (ECG) sensor to observe the biosignals. For establishing the biodata analysis framework, OHPAS initiates the fusion of Variable Auto Encoder (VAER) and K-Means clustering techniques. This phase comprises dataset feature reduction, data regularization, and clustering operations to make the dataset effective for the training process. Finally, the Long Short Term Memory network (LSTM) uses the preprocessed dataset for computing the training dataset. The proposed OHPAS contributes novel features such as a real-time patient monitoring environment, effective sensor data reduction, distributed sensor data analysis, day-wise PD symptom prediction, reactive PD alerts, and accurate early detection solutions. Considering effective medical data analysis with minimal response time, the proposed model creates reactive body sensor network. Under this sensor platform, sensor modules contain proposed DL procedures in its internal memory for initiating data analysis practices. Consequently, the symptoms of PD are commendably detected and predicted with minimal response time. The experimental results indicate the proposed PD system outperforms the existing systems with 8% to 10% of better results.

INDEX TERMS Parkinson's Disease, body sensors, neural networks, deep learning, PD symptoms and healthcare.

The associate editor coordinating the review of this manuscript and approving it for publication was Theofanis P. Raptis.

I. INTRODUCTION

Parkinson's Disease (PD) has many notable and measurable symptoms. The common symptoms of PD are shaky

movements, slowness in body movements, difficulty in walking, and speech disorders. Other psychological symptoms like anxiety, stress, depression, behavioral issues, and sleeping issues are common among many PD patients. Especially, the PD-affected patients get abnormal facial expressions due to the loss of control in their facial muscles. Since many body syndromes rise due to various reasons, determining the symptoms of PD is a challenging task.

At the same time, the classification of PD symptoms make a crucial role to identify the growing stages of PD. Body sensors play a major role in live PD analysis frameworks. In this case, a detailed study is essential to determine PD's severity, symptoms, stages, and therapy solutions. PD is classified into five stages. During the initial stage, a person feels mild symptoms without affecting the daily routines. In this stage, movement irregularities and tremors raise on any one side of the human body. The initial stage symptoms are not accurately determined by medical practices. From this stage, the severity of PD grows gradually and affects the patient's activity badly.

Finally, PD creates major disorders in movement characteristics, psychological characteristics, neurobehavioral characteristics, sensory characteristics, and other biological characteristics. The growing rate of PD is not predictable unless we develop a highly trained PD symptom analysis system. Generally, the symptoms of PD are classified into two categories. They are motor symptoms and nonmotor symptoms. Motor symptoms specify the actions like tremors, rigidity, and other muscle disorders. These include movement irregularities. Nonmotor symptoms contain speech disorders, eye problems, sleeping issues, and others. Bradykinesia is one of the main symptoms of PD that leads to sluggish physical activities. Bradykinesia is initiating movement disorders gradually throughout the human body. This creates a lack of muscle-based movement activities and a lack of body part coordination.

Clinical measurements and computerized techniques are widely used for the early diagnosis of the symptoms. The crucial symptoms of PD are muscle rigidity (stiffness), imbalanced conditions, tiredness, muscle pain (dystonia), abnormal facial expressions, voice disorders, memory disorders (dementia), sleep disorders, sensation disorders, and urinary bladder weakness [1], [2]. Based on the symptoms of PD, risk factors vary according to gender, age, and toxin exposure. Particularly, age plays a major role in producing the biggest risks for brain disorders. Clinical experiments and diagnosis tools help to detect the symptoms of PD. Clinical practices such as blood testing, Computer Tomography (CT), Magnetic Resonance Imaging (MRI), and Positron Emission Tomography (PET) are globally taken against PD. The clinical tests deliver significant results for taking decisions to save a PD patient's life.

Usually, the reduction in the dopamine level of the brain initiates the PD symptoms. In this case, the medicines treat the regular dopamine levels to induce the necessary biological actions. Similarly, the dopaminergic drug improves the muscles' flexibility and reduces stiffness and tremors. However, PD is not a completely treatable disease [3]. Under the given medical solutions, levodopa is the most effective drug for PD. This drug is available in capsule and liquid form. This drug induces the brain cells to extract dopamine levels. Generally, the drugs maintain dopamine levels [4], [5]. Notably, Monoamine-oxidase B inhibitors (MAO-B) are the substitute drug for levodopa. As MAO-B abolishes dopamine, it affects brain activities.

The inhibitors restrict MAO-B to activate the brain for more time. This drug contains selegiline and rasagiline. MAO-B inhibitors take the effort by resisting the causes of MAO-B in the brain. On the other end, surgeries are required for the particular patient to be recovered. Deep brain stimulation is a surgery to embed the electrodes in the brain. It helps for solving the neurological disorders caused by the brain diseases. The deep brain stimulation surgery saves PD patients from severe problems. In this connection, Thalamotomy is initiated for treating the tremors of PD patients. This therapy destroys or eliminates the particular part of brain cells called the thalamus. Similarly, many surgery solutions are recommended based on the patient' need [6], [7].

Apart from tremor and stiffness symptoms, PD gradually affects human vocal activities. The quality of speech consists of frequency variations, voice pressure, signal strength, and noise levels. Human voice characteristics are classified using the spectral properties of each PD patient. This practice is used to differentiate PD patients' voice irregularities. PD disturbs the speech qualities and clarity of the vocal system. Many computerized techniques develop vocal diagnosis systems. These techniques help to extract the voice properties and signal factors of PD patients. In speech analysis, voice delay is considered as a major factor in detecting PD symptoms. Based on these observations and determinations, PD patients can be allotted for respective medical treatments. However, these clinical tests and results are expected to be improved with intelligent decision-making algorithms.

The recent computational health systems develop body sensor networks and Internet of Things (IoT) circumstances to monitor patients' daily activities [8]–[10]. In this medical era, ML and DL techniques help to improve decision accuracy in any platform. Many research works had been developed for diagnosing the symptoms of PD using medical practices and computerized techniques. Any computerized PD diagnosis technique needs suitable PD dataset features (knowledge base) and effective samples to train the decision-making system. The datasets play a crucial role in PD detections and predictions. The recent PD diagnosis technologies mainly use computerized techniques based on various online PD datasets and clinical datasets.

Grounded on the PD knowledge base, the recent computerized PD diagnosis schemes are developed with ML techniques such as Support Vector Machine (SVM), Bayes Classification (BC), Decision Trees (DTs), Self-Organizing Map (SOM), Random Forest (RF), and others for detecting the symptoms of PD. At the same time, DL practices

encompass Deep Neural Networks (DNNs), Convolutional Neural Networks (CNNs), Recurrent Neural Networks (RNNs), Auto Encoders (AEs), Deep Boltzmann Machines (DBMs), and Generative Adversarial Networks (GANs) for classifying the symptoms of PD. Compared to conventional PD diagnosis models, the recent ML and DL techniques provide better diagnosis results.

The accuracy of ML and DL-based PD diagnosis models varies with respect to their learning rates. The learning rate and the accuracy rate of any ML or DL technique are decided from the effective utilization of the knowledge base. Under this circumstance, the integration of IoT-based body sensor networks and the DL networks ensures live PD monitoring possibilities. In addition, a properly designed DL network with a regulated knowledge base accurately analyzes the live biosensor data to detect the symptoms of PD [11]–[13].

The research works developed a computational PD diagnosis system using patient health records. Under the DL frameworks, PD diagnosis models create well-trained systems for implementing PD data evaluation procedures. The results generated from DL reveal the optimal contributions in PD data analysis platforms. On the other hand, body sensor networks are used to observe the real-time bio measurements to alert the patients [14]–[16]. In contrast, the existing PD diagnosis models are limited to nonlinear data manipulations, dimensionality reductions, and reactive PD analysis practices. Additionally, the recent PD diagnosis models are inadequate against optimal dataset management problems, effective time series data analysis problems, real-time sensor handling problems, data regularization issues, and home-based PD monitoring solutions [17]–[19]. These are considered crucial research problems.

To solve these problems, the proposed work develops an effective DL-based PD data analysis models with the help of real-time body sensor networks. The proposed OHPAS monitors various motor and nonmotor symptoms of PD. In this regard, the proposed system is motivated to plant body sensor networks to build independent health monitoring and analysis model to take an effective decision with minimal delay. On the scope of the research problems, the proposed system uses a novel Deep Clustering (DC) technique for effectively managing the PD dataset and training the PD diagnosis system. In this respect, VAER and K-Means techniques are supporting dimensionality reduction and clustering procedures respectively.

On the other side, LSTM takes multi-sensor data streams through various time intervals. The DC mechanism integrates VAER and K-Means approaches with data regularization. In this PD diagnosis environment, LSTM manages multi-sensor data and evaluation procedures for detecting the symptoms of PD. This reactive PD diagnosis environment gets placed in the Raspberry Pi module that is connected with sensor points. Thus, the proposed OHPAS contributes to dimensionality reduction, data regularization, LSTM-based PD symptom detections, and predictions. The contributions of the proposed system are listed below.

- Establishing a deeply trained PD diagnosis environment using body sensor networks
- Analysing motor and nonmotor symptoms
- Detecting and predicting the sensor data anomalies
- Developing a reactive PD monitoring and assisting environment

The article is organized as follows. Section 2 takes notable research works on PD symptoms, data gatherings, clinical data analysis, body sensor networks, medical supports for PD patients, ML and DL-based PD solutions. Section 3 provides technical details, hardware components, and algorithms for implementing the proposed OHPAS. Section 4 shows the real-time experimental setup and performance evaluations. Finally, section 5 states the conclusion and future impression of the proposed system.

II. RELATED WORKS

This section investigates the articles related to PD diagnosis models, ML and DL-based diagnosis models, medical sensor applications, reactive PD monitoring techniques, and disease classification mechanisms. Soumaya *et al.* [1] proposed PD detection techniques with the help of SVM and Genetic Algorithm (GA). This work evaluated the speech signal variations for detecting the symptoms of PD. In this regard, this work created Discrete Wavelet Transforms (DWTs) of multiple voice samples collected from PD patients. Additionally, this system collected frequency samples, voice code samples, and entropy features of voices. Subsequently, ML-based classification techniques such as SVM and GA were applied to the collected datasets. These ML techniques classified the given voice datasets to observe the voice abnormalities of different PD patients. This technique contributed significantly to find the voice symptoms of PD patients. However, this was a conventional technique and it was not producing real-time monitoring benefits. A few other research works discussed the evidence of clinical symptoms and medical therapies given for PD-affected patients [2]–[5].

Bind *et al.* [6] executed a deep comparative study on various ML-based PD detection techniques. This study gave an extensive idea about PD symptoms, PD detection techniques, PD prediction techniques, and experimental evaluations. This work identified different computational techniques such as Artificial Neural Network (ANN), GA, SVM, RF, Naïve Classification (NC), K-Nearest Neighbour (KNN), and various probabilistic models. This study produced effective comparisons between various PD detection techniques. Particularly, the techniques concentrated on speech analysis models and body movement analysis models to detect PD symptoms. Yaman *et al.* [7] developed a PD detection framework using patients' acoustic features. This effort contributed to statistical pooling techniques for classifying and evaluating voice features. Additionally, this PD recognition scheme gathered patients' handwriting samples, gaits samples, and balance factors. In this work, SVM and KNN techniques were producing effective feature classification results. Besides,

this work missed the actual construction of real-time DL structures for evaluating the biological features. In the same manner, Mittal *et al.* [8] and Polat *et al.* [9] proposed notable research contributions for enabling dependable solutions to detect PD symptoms using acoustic measurements.

Under both techniques, voice sampling approaches and conventional ML techniques were used for extracting the notable voice data sequences. In this regard, these works had collected various PD clinical datasets and applied ML techniques to voice features. Anyway, these works produced less data complexity yet these were inefficient to produce more accuracy. Additionally, these techniques are expected to be improved to meet real-time benefits.

Pfeiffer *et al.* [10], Schapira *et al.* [11], and Ba *et al.* [12] discussed various motor and nonmotor symptoms of PD stages. Moreover, these works discussed motor and nonmotor relationships for extracting PD disorders. Grover *et al.* [13] proposed a DL-based PD severity prediction system using ANNs. This work utilized patients' speech abilities, moving abilities, and other natural activities for extracting PD features. This work took online clinical datasets, not sensory datasets. In the same way, Sivaranjini *et al.* [14] developed CNN Based PD Diagnosis System (CPDS). CNN is an effective DL technique for extracting image features with the help of multi-level filter functions. In this work, CNN functions worked on MRI features for extracting the PD symptoms. This work stated that the developed DL technique produced significant results. Compared to other DL techniques, CNN takes minimal training time and processing time [15]–[18]. In this regard, this existing system supported for effective symptoms detection based on MRI data features. At the same time, CNN-based DL techniques were limited to huge dataset quantities, uncertain data correlations, and time-series data extraction.

Nagasubramanian *et al.* [19] proposed Multi-Variant PD Diagnosis System (MVPDS) using DL techniques. This system established PD vocal data analysis procedures and PD detection procedures. This work utilized online PD datasets for training the DL networks such as Recurrent Neural Networks (RNN), CNN, and DNN structures. This work stated that the proposed acoustic-based PD detection techniques produced optimal results. However, this technique was developed using standard Unified PD Rating Scale(UPDRS) data and standard learning models. This approach created learning complexity in terms of data extraction and processing time. Additionally, this work was limited to static online dataset features and it was not developed for real-time sensor readings.

Balaji *et al.* [20] proposed Supervised ML-based PD Diagnosis system (SMPDS) using Decision Tree (DT), Ensemble Classification (EC), SVM and BC rules. SMPDS implemented classification techniques for detecting gait features of patients. In this regard, this system used UPDRS gait datasets to train the ML system. Particularly, SMPDS was developed to analyze vertical ground activities when the patient walks. This system provided a useful and easy way for PD data analysis models. In contrast, this technique suffered from limited accuracy and nonlinear constraints. Diaz *et al.* [21] proposed a handwriting analysis model to detect PD symptoms using one-dimensional convolutions.

This work had a novel idea of using CNN under a single-dimensional data field. This work analyzed sequentially generated handwriting data patterns using convolutional functions. This system gathered various patients' handwriting samples to train the network model. Usually, CNN is a suitable choice for image analysis models. As the handwriting data was taken into convolutional layers, this work gave optimal detection results in the PD diagnosis phase. In contrast, this work handled only limited handwriting samples. In a similar style, Powers *et al.* [22] developed a smartwatch-based PD diagnosis system. This work was implemented with smartwatch-based inertial sensors to monitor real-time patient data. The smart watch-based monitoring scheme contributed to an efficient PD analysis model. As this work used inertial sensors in a smartwatch, the motor symptoms and other movement fluctuations were recorded to detect the symptoms of PD. This work was mainly designed for monitoring tremor issues and dyskinesia presence. Anyhow, this system had limited technical benefits in the training section and it was not adaptable to DL approaches to improve the PD detection rate. Similarly, Mirelman *et al.* [23] proposed mobility feature detections. This scheme used standard ML techniques such as feature selection, classification, and clustering approaches. The techniques provided nominal observations on PD detection. However, this work had no features of DL-based feature selection and clustering techniques to improve the quality of the PD data analysis model.

In general, recently developed PD diagnosis systems found clinical and online datasets for detecting the symptoms of PD. The existing research contributions are good enough for finding the symptoms of PD [24]. The existing systems developed various models for detecting PD stages using different biosignal measurements. Anyhow, most of the research works collected huge datasets without considering lower dimension possibilities. Additionally, they lacked to tune and regularise the dataset which is a necessary step for maintaining optimal neural network functions. This effort makes a crucial impact on the PD decision-making system. On the other hand, the need for building a handheld PD analysis system is inevitable. In this state, the proposed work is interested to develop a modest and effective OHPAS for helping PD patients in their homes. The sensors used in this work collect the biological data from patients' body parts and deliver the data to DL computational block. This computational module holds efficient and lightweight DL techniques to evaluate the sensor data to ensure the real-time severity level of PD. The technical details of the proposed OHPAS are given in section 3.

III. PROPOSED SYSTEM

The proposed OHPAS contains the necessary technical components and novel DL techniques for detecting the symptoms of PD at the earlier stages. This system integrates body sensor

environment and computer diagnosis environment to build effective PD monitoring and assisting equipment. The proposed system has the following implementation phases.

- Deploying the body sensor computing environment
- Implementing the proposed data handling Techniques
- Building a comparative experimental testbed

A novel PD monitoring and assisting system need a suitable computing environment for getting real-time responses. This computing environment shall comprise a tiny processor, inbuilt volatile memory or Random Access Memory (RAM), Read-Only Memory (ROM), General Purpose Input and Output System (GPIO), interfaces, Wi-Fi (Wireless-Fidelity) module, Bluetooth module, the rechargeable battery unit and body sensors. This environment helps to sense the biological objects related to motor and non-motor activities. At the processing end, the medical data is evaluated to detect the symptoms of PD. The processor unit of OHPAS works with different DL techniques such as VAER, K-Means clustering technique, and LSTM to classify the symptoms of PD. This practice aids to build an active and automatic decision-making system against PD.

TABLE 1. Body sensors and computing environment.

Devices	Device Details
MC-10- (Accelerometer, gyro sensor, ECG and EMG)	MC-10 with volatile memory unit and Bluetooth
Microphone Acoustic sensor	MC-1500 (30 dB), UT-PF Sensor
Processor	Raspberry Pi - V4 - B (BCM 2711, Quad-Core A72-64 Bits)
Connectivity	Wireless 802.11 ac, Bluetooth 5.0, GSM module
Relays	Wired and Wireless interfaces
Datasets	Clinical Datasets, Biosensor Datasets and UPDRS Datasets
Phone	Smart phone with investigator application

A. DEPLOYMENT OF SENSORS AND COMPUTING ENVIRONMENT

The proposed OHPAS places a body sensor network that contains the collection of medical sensor patches fixed on human skin. The externally patched sensors observe the live biosignals of a particular patient during regular activities. The proposed system uses various body sensor units to monitor both motor and nonmotor symptoms of PD. MC-10 is an inertial multi-sensor unit that contains an accelerometer sensor, gyro sensor, ECG, and EMG modules as a single patch. This sensor unit monitors the patient's hand movements, leg movements, angular movements, and cardiac variations respectively. Particularly, the accelerometer sensor observes the data of external body movements. The Gyro sensor reads the biodata of angular movements and velocity of a particular activity. Similarly, EMG gets the data of muscle and nerve activations [25]–[27]. These are called as motor symptoms related to body movements. In the same manner, ECG records heart pulse readings.

MC-10 sensor unit has inbuilt Random Access Memory (RAM) for storing real-time patient data. It has a Bluetooth module to transfer the data to any nearest Bluetooth-enabled system or cloud network. Additionally, it is available with a multi-sensor charger unit. This sensor unit is rechargeable at any time. MC-10 senses and delivers the bio measurements to any computer system [28]–[30]. In addition to MC-10 sensor patches, this system uses MC-1500 (30 dB) microphone and UT-PF sensors for observing the patient's voice features. These two devices are also patched sensors to be fixed on the patient's neck skin (nonmotor symptoms). The technical details of the sensor units are given in section 4. Table 1 shows the body sensors and other hardware details. The proposed PD monitoring system uses multiple MC-10 units and acoustic sensor units to observe the real-time data sequences. PD monitoring and decision-making system need effective data evaluation procedures to detect the symptoms correctly. Under the data analysis phase, data extraction, data modelling, data analysis, and decision support are the major actions. The actions related to data processing and data computation shall be executed by any computing devices. In this regard, the proposed system deploys Raspberry Pi Version 4 (Model B) for installing and initiating the DL routines over body sensor data streams.

The deployed microprocessor module has wired network protocols, wireless network protocols, General Purpose Input and Output (GPIO)- 40 pins, and power units. Additionally, this processor unit has 4 Gigabyte (GB) of RAM with a 64-bit processing core (ARM-Advance Reduced Instruction Set Computer Machines). Also, this unit has Raspbian-Noobs operating system, expandable storage card slots, and universal serial ports. The PD diagnosis and assisting environment needs additional interfaces (relays), a smartphone with a data visualizer application, and the deployed DL procedures with training datasets. This complete environment helps to sense and analyze the data to generate the PD decision reports [31], [32]. Usually, DL networks get structured inputs to be processed for detecting the symptoms of PD. Mostly, the sensors produce a sequence of unstructured data. This data sequence shall be regulated using appropriate data models discussed in the next section.

B. IMPLEMENTING DL TECHNIQUES FOR DETECTING THE SYMPTOMS OF PD

As discussed, the proposed DL techniques analyze the patient data sequences collected from different sensors.

In this work, acoustic sensors and motion sensors play a major role in the data acquisition phase. Acoustic sensors create a sequence of raw voice measurements that should be structured using a suitable phonetic or acoustic model. At the same time, other sensors generate the biosignal measurements dynamically. An appropriate mathematical model stabilizes the sensor data under time series circumstances. An acoustic sensor produces time series values of frequencies and amplitudes. The real-time sensor values need to be gathered using the proper acoustic data model. In this regard, Dynamic Phonetic Model (DPM) calculates the resemblance and difference of speech signals. DPM allows the proposed system to compare two speech signals and detects the similarities of signals in time domain. The basics of DPM are formed by calculating the distance matrix between dual time sequences. In this regard, DPM computes the spectral distance matrix to differentiate the series of acoustic events. Additionally, the model ensures the regulated flow of sensor data into DL networks. Equation (1) illustrates the acoustic time series model. This dual-time series data pattern shall be integrated into the input layers of DL architecture. Equation (1) denotes the difference in acoustic sensor measurements through DPM. $S^{ti(x)}$ and $S^{tj(x)}$ denote the voice observations of a particular patient at time *ti* and *tj* respectively.

$$S^A = \sum \left| S^{ti(x)} - S^{tj(x)} \right| \quad \forall \mathrm{n} \tag{1}$$

$$DS^A = \sum \left| S^{ti(x)} - S^{tj(x)} \right| + \min(c) \tag{2}$$

Let, c is the collected acoustic readings at various durations. Equation (2) gives the optimal forward dynamic programming models for feeding the time series acoustic patterns into the DL network. DS^A denotes optimal acoustic distance measured between two observation points. This model uses to find the closest distance between various dual-point measurements. At the same time, this is not a training model to obtain the optimal decision on PD acoustic readings [33], [34].

On the other side, MC-10 patches generate data from different sensors (accelerometer sensor, gyro sensors, ECG, and EMG). As multiple MC-10 units are stamped on the patient's skin, the identification of a particular MC-10 unit is a significant task [35], [36]. MC-10 sensor units' data are represented as given in equations (3), (4), (5), (6), and (7). Additionally, the recursive optimal function computes forward acoustic patterns using feed-forward dynamic programming solution.

$$M(S) = M^i(S^{ACC}, S^{GYS}, S^{EMG}).\frac{d\tau}{dt} \quad \forall i \tag{3}$$

$$S^{ACC} = S^{ACCi}(m^1, m^2 \ldots .m^k).\frac{d\tau}{dt}\forall i \tag{4}$$

$$S^{GYS} = S^{GYSi}(m^1, m^2 \ldots .m^k).\frac{d\tau}{dt}\forall i \tag{5}$$

$$S^{ECG} = S^{ECGi}(m^1, m^2 \ldots .m^k).\frac{d\tau}{dt}\forall i \tag{6}$$

$$S^{EMG} = S^{EMGi}(m^1, m^2 \ldots .m^k).\frac{d\tau}{dt}\forall i \tag{7}$$

Equation (3) gives i^{th}MC-10 sensor data sequence, $M(S)$contains accelerometer sensor data, S^{ACC}, gyro sensor data, S^{GYS}, ECG data,S^{ECG} and EMG data, S^{EMG}. The patient can hold $'n'$ MC-10 sensor patches on patient's body. The sensor data is collected in time series manner where the current time is, $'\tau'$. Similarly, equation (4), (5), (6) and (7) show the individual accelerometer, gyro sensor, ECG and EMG sensor data. The time series sensor measurements are denoted as m^k. In this case, $M(S)$ is considered as primary data tuple (quadruplet) that has all inertial sensors. Thus, the sensors collect the data for ensuring patient's stress, muscle irregularities, tremor and voice distortions. Particularly, the patient can do any activities by wearing the sensor patches. Figure 3 shows the block diagram of OHPAS. Predominantly, body sensors are connected with Raspberry Pi (Bluetooth connection). On the other end, Wireless Fidelity (Wi-Fi) or Global System for Mobile Communication (GSM) protocol shall be taken for communication control. The selection of communication protocols varies based on the distance between the modules.

Figure 2 illustrates the body sensor stamp points fixed on human body and the Raspberry Pi belt. MC-10 sensor patches are fixed at the chest, muscle parts of hands, legs, shoulders, and wrists. The inertial sensors shall be fixed at different body parts to detect the movements and muscle distortions. At the same time, the UT-PF sensor patch and microphones shall be stacked at the neck portion of the human body. As shown in Figure 2, a body sensor environment is deployed to collect the biosignal measurements of PD patients [37], [38]. Similarly, the acoustic sensor patches record the patient's voice data. The data collected from distributed sensor patches are given in to Raspberry Pi. As mentioned in Figure 2, the Raspberry Pi module has been fixed with a hip belt to gather and analyze the multi-sensor data. In this deployment, the Raspberry Pi unit has data analysis procedures for detecting the symptoms of PD using multi-sensor data. As the sensor patches transfer the data into the Raspberry Pi module using Bluetooth protocol, the following DL procedures and training models are called by the computing module [39], [40]. In this case, RNN is a deep neural network used for taking decisions on time series data analysis models.

RNN is a feed-forward neural network that maintains internal memory cells. RNN gets the sensor input data and computes outputs based on previous computations. Generally, RNN's output function depends upon previous decisions. In this regard, the computations of each iteration are delivered back as the input function of RNN. RNN holds its internal memory states to keep previous computations for producing next state outputs.

In RNN, the internal functions are configured with relative input conditions. This unique quality of RNN helps to analyze the multi-sensor data for detecting the symptoms of PD. Unfortunately; the basic RNN has gradient problems and exploding problems that affect the real-time decision-making process. In this situation, the LSTM network solves the problems produced under standard RNN. LSTM has a

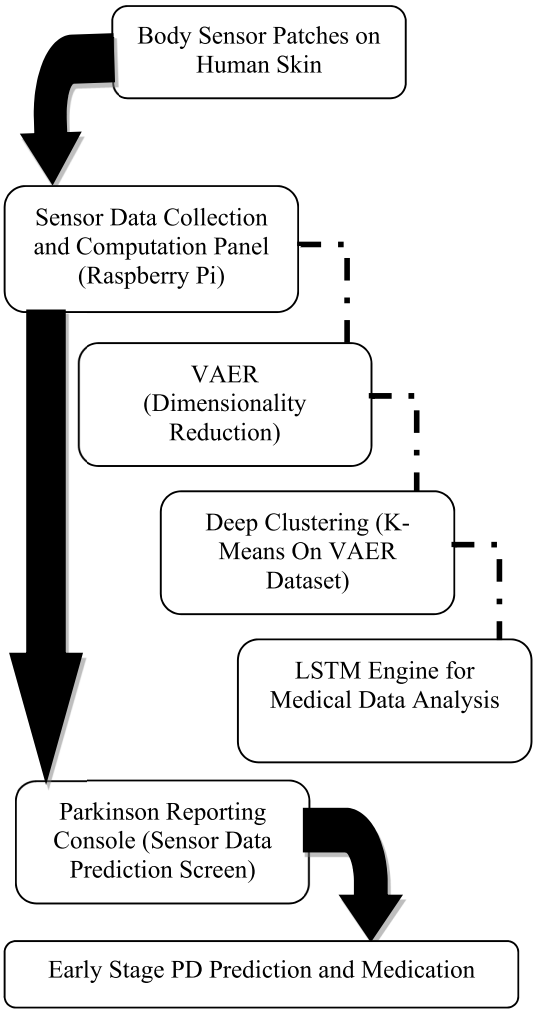

FIGURE 1. OHPAS modules.

back-propagation training model to train the network to investigate the PD data. The proposed system constructs the LSTM training dataset using clinical PD measurements, biosensor datasets, and UPDRSs.

The proposed system has been modelled with the sensor data propagation in a structured time series pattern [41]. As discussed, the Raspberry Pi processor module receives the MC-10 and acoustic sensor data sequences via Bluetooth interface. The structured input series get placed into DC enabled Raspberry Pi unit.

The proposed system manages multi-variate sensor data. The accuracy of any decision-making model depends on dataset optimization policies and training policies. At this point, the proposed DC plays a crucial task in regulating the raw dataset for effective experimental usage. This process enhances the accuracy rate of the proposed PD diagnosis system. The proposed technique has three major components such as VAER architecture, K-Means clustering technique, and LSTM architecture. VAER and K-Means approach initiate dimensionality reduction and clustering benefits respectively. On the other hand, LSTM initiates recurrent training

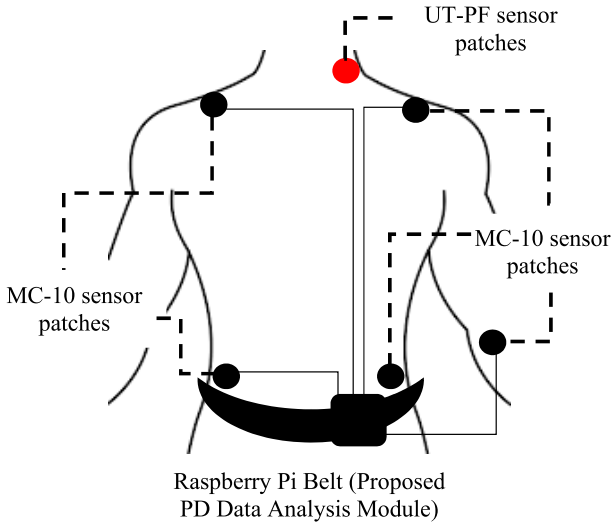

FIGURE 2. Body sensors patches.

procedures for detecting the symptoms of PD. In this proposed model, both LSTM network and VAER based K-Means clustering generate lower dimensional dataset with minimal loss. The loss rate is classified as network loss (LSTM) and clustering loss (VAER/K-Means). Equation (8) illustrates the loss rate that states nonlinear sequence of unsupervised learning loss rate [42], [43].

$$DC^{L} = L^{LSTM}.\alpha + L^{CL}(1-\alpha) \tag{8}$$

In this equation, cluster loss, L^{CL}, states both VAER loss and K-Means loss (cluster assignment loss rate and cluster tuning loss rate). As mentioned, the proposed system uses LSTM network architecture for PD data evaluation. However, the LSTM model needs more accurate samples to train the network [44]. The network loss is defined as L^{LSTM}.

The weight term α *is* used to adjust the overall network function. The proposed novel structure helps to train the PD dataset and evaluate the sensor readings. Generally, AEs work on huge random datasets and reduce the data dimensions in to lower range. The nature of AE eliminates data redundancy, missed data and noise in given complex dataset.

Accordingly, the fusion of VAERs and K-Means procedures executes effective clustering in lower dimensions and creates clustered data points respectively. This proposed system builds VAER for handling dimensionality reduction and generating new samples from the latent space. The new sampling phase improves the classifier accuracy and clustering quality. The objective function of VAER is determined as given in following equations (9), (10) and (11).

$$E^{VAER(x)} = \sum_{i=1}^{n} P(z|x^{i}) \tag{9}$$

$$S^{VAER(z)} = \sum_{i=1}^{n} z \sim P(z|x^{i}) \tag{10}$$

$$x \sim = \sum_{i=1}^{n} d(z) \tag{11}$$

$E^{VAER(x)}$ denotes encoding process of VAER at the latent space,z(initial probability distribution of all x^i). $S^{VAER(z)}$ denotes the sample data point taken from initial distribution in to latent space z. $x \sim$ illustrates reconstructed data of decoder function $d(z)$ from the latent space z. The data samples are brought in to the latent space to tune the decoder function. This scheme works for reducing the data dimensionality and generating new values. In this case, the latent space is defined as the space where the data is compressed and encoded. Obviously, VAER produces lossy compression and reconstruction loss. VAER loss function is expressed as given in equation (12).

$$VAER^{LOSS} = \|x - x \sim\|^2 + KL[N(m^x, c^x, N(0, I)] \tag{12}$$

$$VAER^{LOSS} = \|x - d(z)\|^2 + KL[N(m^x, c^x, N(0, I)] \tag{13}$$

In equations (12) and (13), x is the original data. KL denotes data regularization component that is expressed using Kullback-Leibler Divergence between Gaussian distribution and return data distribution [45]. This is computed with the help of normally distributed mean matrix and covariance matrix, m^x, c^x respectively within the specified numerical range. Let assume, C^P, CO^P are data continuity point and data completeness point respectively. As shown in equation (12), $x \sim$ is the reconstructed data. KL divergence has been computed over the mean input components and variances under the normalized conditions.

In addition, $N(0, I)$ denotes the range of normalized values during previous iteration. In this case, I denotes the highest normalized probability change. The loss function computes the significant variance during data encoding and reconstruction phases.

The purpose of VAER computation is to observe the complex data loss rates while VAER executes encoding and reconstruction procedures. This computation helps to measure and control the dimensionality reduction rate of VAER network.

VAER regularises the complete encoding and decoding processes based on data continuity point and data completeness points. Notably, the closer continuity data points, C^{Pi}, CO^{Pj} may not produce different generative item at the reconstruction end. At the same time, the sample data point from the latent space z gives crucial content at the end of decoding process to the classifier. The main goal of VAER is expressed as shown in equation (14).

$$VAER(e, d) = \min(VAER^{LOSS}) \quad \forall z.d\tau \tag{14}$$

The main use of VAER is to reduce and data dimensions and produce new contents from the latent space that impacts decoder generative function to produce less errors comparing to other AEs. Figure 3 shows the functional blocks of VAER. The proposed system assumes that the VAER produces minimal reconstruction loss with optimal data reduction rate (compression rate). The reconstructed data features are computed using K-Means clustering algorithm to build relevant

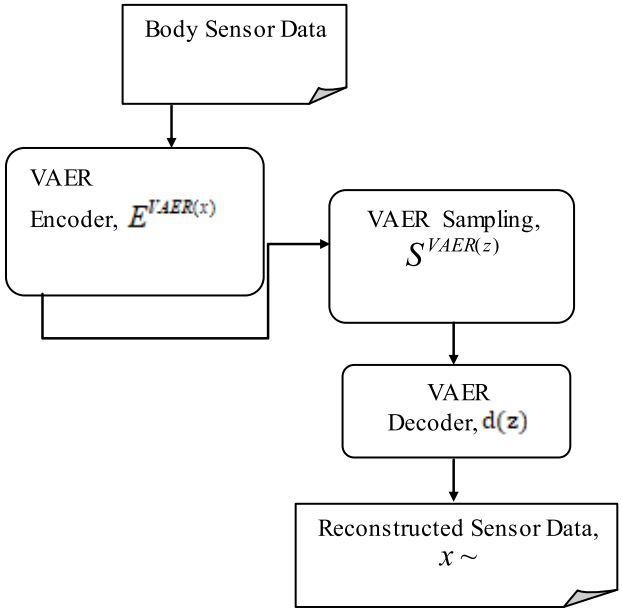

FIGURE 3. Basic blocks of VAER.

feature groups. K-Means associated VAER is determined as illustrated in equation (15). In equation (15), c, n are number of clusters and number of cases correspondingly.

The case of VAER data can be denoted as, $x \sim_i^j$ and the centroid of cluster is C^j.

$$DC(x) = \sum_{j=1}^{c} \sum_{i=1}^{n} (x \sim_i^j - C^j)^2 \tag{15}$$

The clustering loss component can be defined as $L^{CL}(1-\alpha)$ from equation (8). The network loss component is defined as, $L^{LSTM}.\alpha$ from equation (8). As discussed in equation (8), the overall loss rate, DC^L contains both LSTM loss rate and clustering loss rate. Equation (15) shows deep clustered output, $DC(x)$ that produces the loss rate of $L^{CL}(1-\alpha)$. Now, the need for LSTM principles is mandatory with this deep clustered output features, $DC(x)$. As discussed earlier, LSTM suits for analysing time series data coming from different sources where the dataset is effectively regularised and reduced. Algorithm 1 shows VAER/K-Means based clustering phase and LSTM training phase for detecting the symptoms of PD. This algorithm gets data from MC-10, UT-PF and MC-1500 sensors continuously. As it maintains reduced and clustered dataset (VAER/K-Means), LSTM trains itself to produce training dataset and test dataset iteratively to tune the decision network. LSTM is a recurrent type neural network to compute the current output from current input data and previous computations. This practice keeps previous sensor data in its internal memory and produce recurrent computations. In this regard, the proposed system detects and predicts the PD measurement series [46], [47]. This task improves PD detection accuracy rate and supports early detections of PD. Algorithm 1 illustrates the proposed OHPAS functions and

Algorithm 1 DC and Real-Time PD Diagnosis

Input: PD Raw Dataset, S^{ACC}, S^{GYS}, S^{ECG}, S^{EMG}, DS^{A}
Output: Reports on PD Symptoms (Smartphone)

1: Initialize DC (K-Means based VAER network)
2: Get PD dataset (Raw contents)
3: VAER Encoding and Sampling
Call $VAER(e, d)$ as $E^{VAER(x)}$, $S^{VAER(z)}$
4: VAER decoding and reconstruction
Call $x \sim$ as a collection of reconstructed data points
5: Do K-Means clustering, Call $DC(x)$ over$x \sim$
6: Determine both K-Means loss, VAER-Loss

$$L^{CL} = K^{LOSS} + VAER^{LOSS} \tag{16}$$

7: Generate a clustered dataset items, $DC(x)$
8: Initiate LSTM training model, T^{LSTM}
Get the data items from $DC(x)$
Generate sample training dataset, $Tr(x)$
Generate Test dataset, $Tt(x)$
Do feature selection
9: Train the LSTM and Tune the LSTM iteratively to Get minimal, L^{LSTM}
10: Get real-time data sequences from body sensors
11: Test the sensor data with LSTM's $Tr(x)$ and make recurrent computations and update LSTM memory
12: Compute iterative results and predict the sensor readings at $d\tau$.
13: Send reports to smartphone investigation application

outcomes. The construction and working details of LSTM is given below.

Let assume a trained LSTM has minimum network loss rate, min(L^{LSTM}). LSTM has three gates such as input gate, $G^{I}f$orget gate, G^{f} and output gate, G^{O}. It has crucial layers like, candidate layer, C^{LCAN} and hidden layer, H^{L}. The internal memory cell or state is denoted as C^{M}. Let assume, LSTM cell at current time gets input sensor data from any sensor, $S^{i(\tau)}$. The previous hidden cell state is denoted as τ. $H^{\tau-1}$ and previous memory cell state is given as $C^{m(\tau-1)}$. The current LSTM output has two terms such as, current hidden cell state, H^{τ} and current memory cell state,. Apart from three LSTM gate units, candidate layer, C^{τ}. C^{ct} of LSTM plays tangent function on hidden layers.

$$G^{f} = \sigma(S^{i(\tau T)} * I^{f} + H^{\tau-1} * \omega^{f}) \tag{17}$$
$$C^{ct} = \tanh(S^{i(\tau T)} * I^{C} + H^{\tau-1} * \omega^{C}) \tag{18}$$
$$G^{I} = \sigma(S^{i(\tau T)} * I^{i} + H^{\tau-1} * \omega^{i}) \tag{19}$$
$$G^{O} = \sigma(S^{i(\tau T)} * I^{O} + H^{\tau-1} * \omega^{O}) \tag{20}$$
$$C^{M(\tau)} = G^{f} * C^{M(\tau-1)} + G^{I} * C^{ct} \tag{21}$$
$$H^{\tau} = G^{O} * \tanh(C^{M(\tau)}) \tag{22}$$

Equations (17), (18), (19), (20), (21) and (22) denote the LSTM's recurrent computations and memory updates. The parameter $S^{i(\tau T)}$ denotes current input vector and σ states sigmoid function. The weight vectors of various gates on both input state and hidden state are denoted as I, ω respectively. In this regard, the LSTM computes current memory state, $C^{M(\tau)}$ from following computation, equation (23).

$$C^{M(\tau)} = G^{f} * C^{M(\tau-1)} \tag{23}$$

The current memory state shall be calculated from forget gate or input gate. The forget gate, G^{f} produces the values between 0 and 1. Let take, completely forgotten previous memory state as $G^{f} - > 0$ and completely passed previous memory state as $G^{f} - > 1$.

The proposed PD data analysis principles (VAER, K-Means, and LSTM) effectively utilize the complex PD dataset. Firstly, K-Means and VAER networks generate an effectively compressed dataset with lower dimensionality PD features from the raw dataset. Thus, the proposed OHPAS ensures both dimensionality reduction and effective clustering using VAER/K-Means procedures. Secondly, LSTM observes the deeply clustered dataset for initiating the training process and tuning process. At the end, LSTM develops an optimally trained recurrent learning model for analyzing the multi-sensor data [48]–[50]. The proposed body sensor system works with multiple sensors and in-memory DL procedures. As the part of decision support phase, the successive PD reports and alerts assist the patient's regularly during their regular activities. A simple report panel delivers the PD symptoms and early detection support to the patient. The OHPAS uses reactive DL structures (VAER, K-Means, and LSTM) that support quick PD detection and PD prediction solutions. The real-time body sensor networks and the DL-enabled computing environment ensure a patient-friendly environment. The implementation details and experimental setup of OHPAS are given in section 4.

IV. EXPERIMENTATION AND PERFORMANCE ANALYSIS

The experiment contains two phases such as input phase and data processing phase. In the input phase, we collect body sensors' (accelerometer sensor, gyro sensor, ECG, EMG, acoustic sensor and microphone) data in to processing module [51], [52]. In the processing phase, we investigate the datasets and process the sensor data using proposed DL procedures. At the end, the PD reports are generated for detecting the early stage symptoms of PD. Table 2 illustrates MC-10 accelerometer observations belong to the single person at various time intervals. The values tabulated show the input details of respective sensor. In this section, $P^{\tau}_{\alpha i}$ denotes the observation time intervals, τ. Table 2 shows accelerometer data as effective amplitude, $e_{v}(volts)$ and frequency magnitude$f$. The tabulated values are considered as mean values during observation time.

Similarly, Table 2 shows accelerometer's movement coordinates (points) in various dimensions (*x axis, y axis and z axis).*

Figure 4 and 5 show the data sequence of accelerometer sensor at different time intervals. Figure 4 illustrates the movement coordinates *(x-axis, y-axis and z-axis)*. Figure 4 justifies the horizontal movements, vertical movements, and third-dimensional movements are varying heavily due to randomly observed muscle disturbances. The stress in the muscles of the particular patient is compared with other people to observe the stiffness based on the accelerometer coordinates. Figure 5 illustrates the effective vibration amplitude (volts) observed during various time intervals (seconds). At the same time, it shows minimum and maximum points of biosignal amplitude generated during the body movements.

In addition, the biosignal amplitude is a vital attribute to record the muscle stiffness of any person.

Figure 5 shows the variation in effective amplitude due to regular movements. This observation helps to identify the minute electronic signal variations that happen during muscle movements. Figure 6 shows the gyro sensor data sequences varying over time intervals τ. Gyro sensor data is represented using either angular velocity (degree/seconds) or vibration amplitude, v. Gyro sensor values appeared in Figure 6 gives the angular velocities with respect to axis based rotations such as pitch, roll, and yaw. This shows the variations of stress in angular measurements at p, r, y activities. Also, Figure 6 shows the mean, maximum and minimum angular velocities observed for a particular person. These values are not common for person with disability and PD patients.

The angular velocities and the accelerometer coordinates are crucially distorted when the movement is initiated by the respective body part (hand, leg, and other parts). Similarly, EMG sensor data is illustrated in Figure 7. It has three pitches of measurement conditions. We have registered the EMG observations at regular time intervals where the people's physical states like relaxation, flexion and semi-flexion. The observations are represented in volts with respect to observation time (seconds). EMG sensor data is illustrated in Figure 7. It has three pitches of measurement conditions. Compared to person with disability, PD patients are not active during flexion states and suffered from tremored stress movements. Similarly, the variations of EMG get uncertain fall and hike for any PD patients. In this observation, EMG recordings are noted for 2000 seconds against different states of each people. Figure 7 illustrates the biosignals of a PD patient. It is normal under relaxation and semi-flexion conditions. However, EMG data varies abruptly during flexion states.

In this condition, a relaxed state indicates minimal muscle movement. A semi-flexion state indicates moderate muscle movements. Finally, the flexion state specifies completely stretched muscle movements of a respective body part. Figure 6 shows flexion state generates frequent amplitude variations with a wide range of values for PD patients.

The collected values are initially classified in order to identify the similarities and deviations. In this regard, body sensor values are manipulated with the help of the Kruskal-Wallis Test. Particularly; MC-10-ECG data sequences of 50 people are evaluated to construct basic sensor data groups. The

TABLE 2. Accelerometer sensor.

Observation Time intervals p_{ai}^{τ} (sec)	e_v	f_m	Movement points		
	v	f	x	y	z
15	0.12	0.44	248	255	290
16	0.18	0.58	256	256	298
20	0.20	0.76	266	260	302
22	0.21	0.88	272	271	311
18	0.15	0.51	235	247	287
19	0.12	0.44	245	256	299
15	0.16	0.53	302	321	333
12	0.24	1.01	333	342	334
10	0.23	1.01	335	345	323
14	0.24	1.17	345	353	329

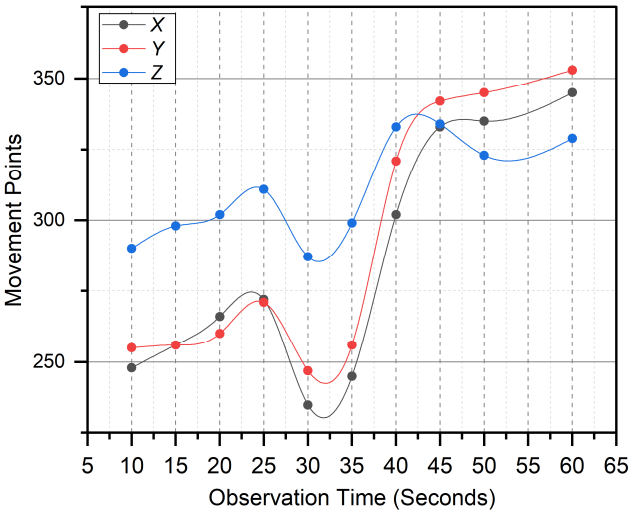

FIGURE 4. Movement observations using accelerometer sensor.

groups of values are manipulated using simple clinical threshold variations and self-similarities. This practice takes Heart Rate Variability (HRV) parameters. Table 3 shows ECG data variations under Kruskal-Wallis testbed. This table shows four groups of ECG data. They are normal values (10), premature variations in values (10), predominant variations in values (15), and controlled values (15). This test is a non-parametric test works based on standard ranking strategies.

It compares the data values and computes the outputs shown in table 3. This gives first-level data impression but not accurate detection of PD categories.

Figure 8 shows the variations in sound pressure (dB) and frequency (Hz) for different people. The acoustic parameters illustrate the observations belong to normal, controlled, premature, and predominant states. Frequency and decibels are directly related to each other. However, Figure 8 notifies the PD patients' incompatible frequency distortions during

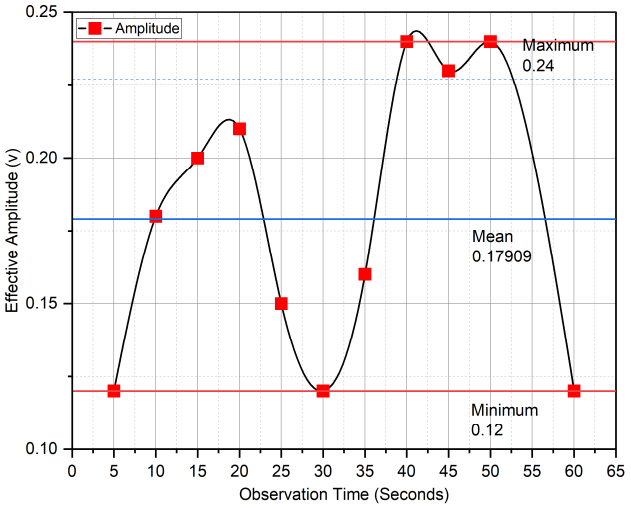

FIGURE 5. Movement stress observations using accelerometer sensor.

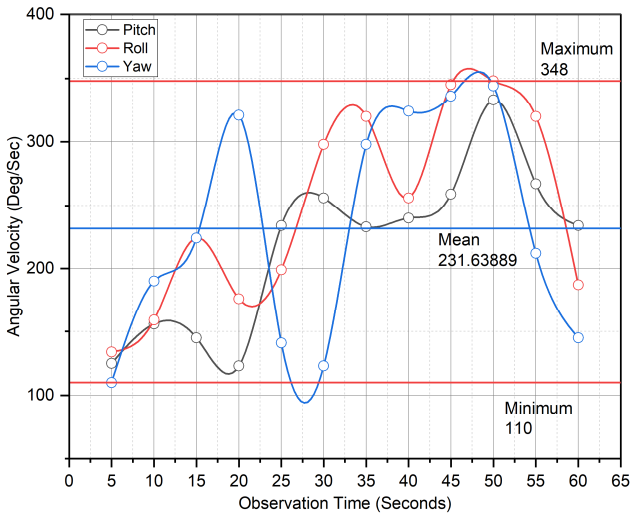

FIGURE 6. Gyro sensor data sequence.

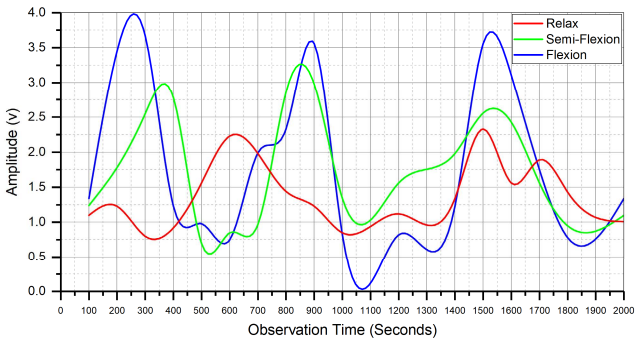

FIGURE 7. Muscle activity observations using EMG sensor.

higher pressure states. The variation is crucial compared to normal and controlled states. The data gathered for 50 different people show crucial variations between sound pressure and frequency at regular observation intervals (seconds). Kruskal-Wallis test uses for baseline data manipulation and similarity identification tasks. This test takes more time to manipulate real-time senor values. Anyhow, the details of sensor data need to be processed under a trained PD diagnosis environment to ensure the exact symptoms of PD stages.

A. DETECTING AND PREDICTING THE SYMPTOMS OF PD USING PROPOSED DC PRACTICES

The sensor data get placed inside the volatile memory of the processor unit and grabbed for DL based PD diagnosis process. As discussed in section 3, the proposed system builds sensor data modeling techniques and deep clustering techniques (VAER, K-Means, and LSTM) for detecting the symptoms of PD. The data collected from different body sensor patches need to be processed efficiently with the help of a trained DL engine. This experiment uses sensory observations to analyze the PD features and stages. In this regard, this work collects the PD datasets from Unified Parkinson's Disease Rating Scale (UPDRS) repositories and clinical reports. Particularly, the datasets contain sound recordings, acoustic features (replicated), tele monitoring features, and other natural speech recordings. The collection of the PD dataset comprises around 7500 instances with relevant features.

The features of the dataset give motor and nonmotor scores, tremors, signal noise, distortions, people's age, sex, and observation classes. The online UPDRS dataset encompasses the data collected from 425 people through different types of experiments. This dataset contains both person with disability and PD patients (male and female). The dataset holds the recordings of the age group between 30 and 90 of both genders. However, the proposed system collects the biosensor data, medical records, and clinical observations of PD symptoms.

The clinical records collected from rural and urban government clinics (India) have 6800 instances of motor and nonmotor data. As same as online dataset, these values cover normal states and PD states. Additionally, the clinical data holds 520 people on both states illustrated above. These clinical data are collected from 21st March 2021 to June 2021 from various neurology centers of clinics. Unlike the UPDRS dataset, the clinical datasets are restricted to research purposes. These datasets are confidential to this PD analysis research work. The integrated dataset has experienced collections of various features. The dataset collected from both UPDRS knowledge base and clinical sectors contain missed data, noise and replications. Also, the total data instances reach 14000 with multiple attributes. The huge size and disconcerting portions of raw dataset create additional overhead during system training and learning steps. In this experiment, VAER preprocesses the dataset to remove all data irregularities and reduce the data dimensionality in to optimal level. The data preprocessing phase include dimension reduction, integration, cleaning and transformation (encoding and decoding) tasks. As the loss rates L^{LSTM}, L^{CL} impact the outcomes of proposed mechanism, training the model with minimal loss rate is an important task. Anyhow, the

TABLE 3. ECG measurements with kruskal-wallis test.

HRV Parameters	Normal (10)	Premature (10)	Predominant (15)	Control (15)
Mean	64.67	66.12	69.43	65.21
SD	2.12	3.95	4.21	2.34
Range	6.85	11.12	11.34	8.21
Coefficient of Variation	3.28	5.97	6.01	3.59
Skewness	0.17	0.02	0.04	0.21
Kurtosis	2.98	2.34	2.44	3.32
Median	64.43	66.14	69.88	65.11

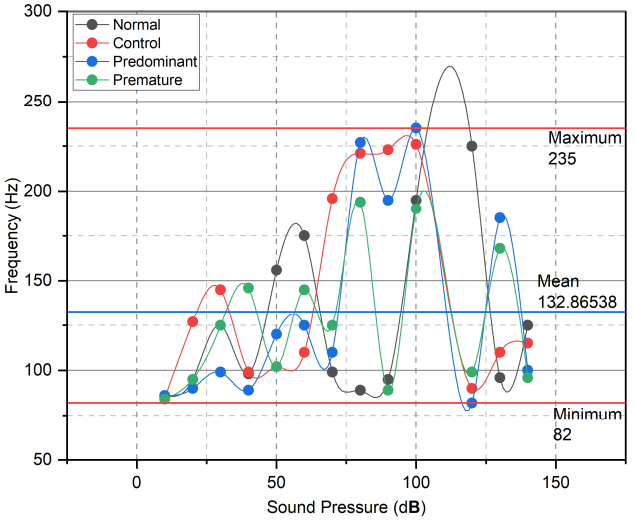

FIGURE 8. UT-PF- acoustic measurements.

proposed VAER works to take deep data preprocessing outcomes.

As discussed in section 3, VAER and K-Means work together for building data quality management and data clustering procedures respectively. Additionally, this phase maintains data regularization and new latent sample extractions to increase the accuracy of disease classification procedures executed by LSTM. Figure 9 and 10 give the benefit of using VAER model over huge PD data collections. Figures 9 and 10 compare the efficiency of VAER based dimensionality reduction over varying instances of experimental dataset with respect to nonlinear correlation factor, C. Many recent works techniques such as Principle Component Analysis (PCA), RF and Expectation Tree (ET), Missing Data Ratio (MDR) and Forward Feature Reduction (FFR) etc. use the dimensionality reduction policies.

Among these techniques, PCA and RF/ET produce crucial impact on dimensionality reduction over vast collection of samples. However, these techniques are limited to data linearity issues. PCA and RF/ET work notably for the homogeneous or linear dataset sequences. On the other hand, they are not effective under nonlinear correlations of data items. The proposed system uses both online dataset instances, biosensor datasets and clinical dataset instances for practicing DL training process. The complex dataset and the samples with nonlinear correlations affect the conventional dimensionality reduction procedures. Consequently, PCA and RF/ET perform equally comparing to VAER under $C = 0.1$ conditions. Nevertheless they fall under $C = 0.4$ circumstance. VAER executes each data preprocessing phases and data sampling tasks. Notably, VAER network reduces the huge set of samples in to lower dimensions with the average reduction rate between 65% to 72%.

On contrast, the VAER reduction rate is slightly oscillated depends on sample nonlinearity issues irrespective to number of samples. However, the performance of VAER dominates other dimensionality reduction techniques under uncertain data conditions. Thus VAER reduces the load of huge data samples in to optimal rate rather than minimal rate. The optimal dimensionality reduction rate of VAER is 5% to 10% higher than other systems. This is determined as optimal reduction state. Particularly, VAER outperforms other techniques for higher number of samples. Additionally, this scheme works efficiently against varying sampling rates. Generally, dimensionality reduction rate impacts clustering loss and cluster computation time directly. VAER executes latent space sampling process once the dimensionality reduction phase is completed.

This sampling process takes runtime samples from the latent space to generate new values to increase the classifier accuracy rate.

As given in Figure 11, the optimal range of dimensionality reduction rate falls between 0.6 and 0.75 that supports better classifier performance with minimal time complexity. This curve justifies the reduction of excessive data from the knowledge base improves the performance of PD data classifier. Yet, the required level of dimensionality reduction rate increases accuracy till the optimal point. The next stage gives the outcome of clustering process that engages both VAER and K-Means techniques. The second phase of clustering initiates the separation of data samples that are reduced by VAER network. The data processed by VAER contains optimal samples without noises, replications or missed data point. Additionally, VAER produces regularized data items as explained in section 3. At the same time, the data are transformed and reconstructed with limited quantity of samples. Clustering of this effective dataset is not a complex task for any standard clustering approach. In this regard, the proposed system uses K-Means clustering approach. Even though K-Means clustering technique is a conventional technique, it gives crucial outcomes with VAER's deeply reduced dataset. Similarly, K-Means reduces the time taken to create clustered data points comparing to other complex clustering techniques.

Figure 12 and 13 illustrate the clusters of data items such as Harmony to Noise Ratio (HNR) and angular velocities

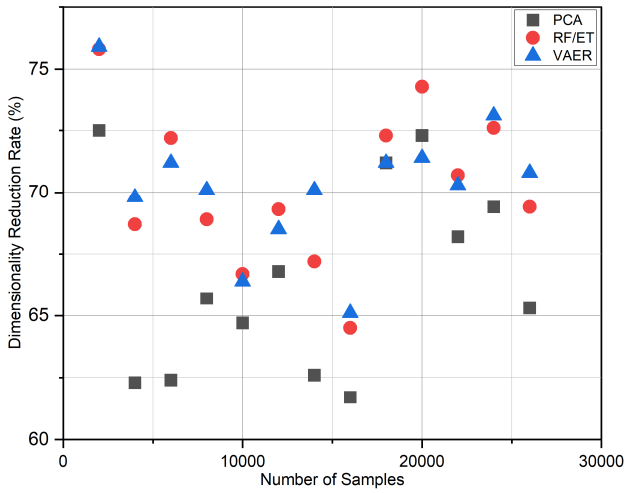

FIGURE 9. VAER and dimensionality reduction $C = 0.1$.

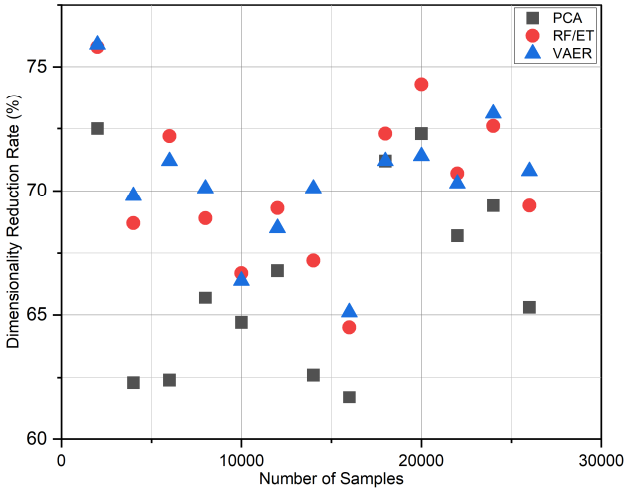

FIGURE 10. VAER and dimensionality reduction $C = 0.4$.

obtained at the end of clustering task (VAER and K-Means). These clustered values are generated from clinical samples and sensor sample of experimental datasets. In the proposed DC, both VAER and K-Means clustering mechanisms work together to reduce the dimensionality and implement the effective clustering respectively. K-Means clustering approach is very simple to group the given data items. At the same time, a simple K-Means algorithm is ineffective against complex nonlinear datasets.

A conventional K-Means algorithm has limitations to deal with huge datasets. On contrast, this simple clustering approach supports for new value generations to build effective clusters. Additionally, K-Means clustering algorithm produces optimal results when the dataset is effectively reduced and preprocessed. In this situation, VAER takes bulk nonlinear dataset (both clinical and online features) to reduce the dimensionality features and transform the same dataset. Figure 12 shows four clusters (normal, PD-Level 1, PD-Level 2, PD Level 3) of people data respectively. In this

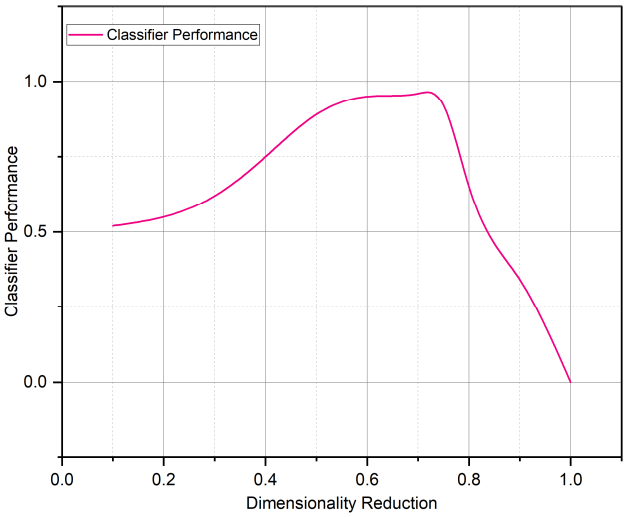

FIGURE 11. Performance relationship curve.

case, the higher PD level indicates more severity level. Similarly, Figure 13 indicates five clusters such as normal, PD-Level 1, PD-Level 2, PD Level 3 and PD-Level 4 orderly. These are preprocessed data clusters obtained from proposed VAER enabled K-Means technique. This clustered dataset is used for training the LSTM layers. In addition, VAER generates newly taken samples from the latent space. The fusion between VAER and K-Means works crucially to generate effective data samples with reduced dimensionality features. In the proposed work, this practice produces only little loss. Figures 9, 10, and 11 are showing the impacts of VEAR based dimensionality reduction process. Figure 12 and 13 provide the optimal clustering solutions. As illustrated in Figure 12 and 13, HNR data points and gyro sensor data points are neatly classified as the original dataset has been effectively reduced.

In the next stage, LSTM helps to build PD evaluation routines with the help of properly reduced and processed knowledge base generated by VAER/K-Means techniques. Consequently, both LSTM network and data clustering technique create minimal data loss during system training phases. Figure 14 depicts the average clustering loss rate and network loss rate with respect to increasing number of epochs.

As mentions in equation (8), (13) and (16), the clustering loss and LSTM loss impact the system performance. However, this loss rate decreases gradually to the minimal rate as the number of epochs attained the satisfaction level. This states that the system reaches the optimal training phases with minimal loss rate.

Figure 14 illustrates the reduction in loss rate over increasing number of epoch (training iterations). The loss rate has been reduced due to iterative recreation of effective samples at VAER state and refining functions of LSTM engines. According to the observations, the optimal number of epochs required to attain minimal loss rate is 250. Thus the PD decision making system has been iteratively trained. Figure 15 shows the OHPAS training time related to number of epochs.

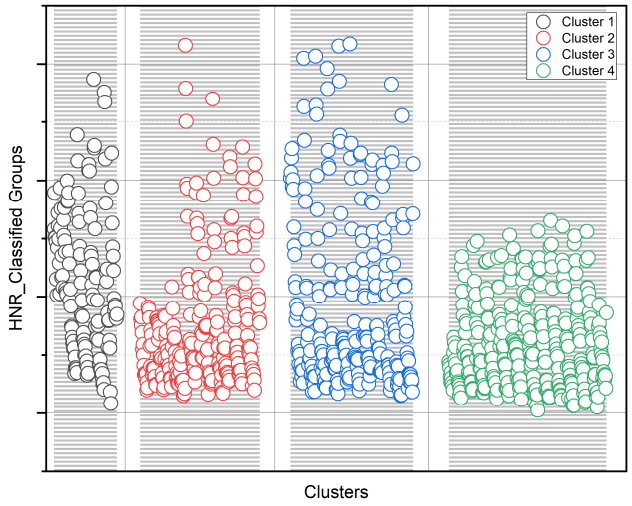

FIGURE 12. Acoustic data features-HNR clusters.

FIGURE 13. Gyro sensor data features.

As the number of epochs reaches 250, the system training time falls to low optimal state. This indicates the successful training completion of PD diagnosis system.

As a part of performance comparison, Figure 16 provides the precision levels of MVPDS, CPDS, SMPDS and proposed system. Generally, the change in the number of epochs directly proportional to system precision rate. The system needs sufficient number of epochs to minimize the decision error. In Figure 16, the precision rate of proposed system varies from 76% to 99.7%. Initially, the precision rate of all PD diagnosis models stays closely. However, the continuous training process leads the system performances in to crucial deviations. The existing systems MVPDS and CPDS used CNN architectures for analyzing the symptoms of PD. Particularly, MVPDS and CPDS analyzed linear acoustic distortions features effectively. Generally, these techniques were implemented for diagnosing acoustic symptoms and MRI features. As number of epochs increases, the training complexity increases with crucial sample quantities. These crucial quantities of PD samples contain both linear and nonlinear correlations with vast distortions.

At this point, the proposed system effectively reduces irrelevant data points and observes effective samples for LSTM layers. Thus the proposed OHPAS works with maximum precision rate (99.7%) at the end (250 epochs). This rate is approximately 10% higher than MVPDS and CPDS techniques. On the other side, SMPDS provides conventional data handling techniques and produce minimal precision rate (74.9%). This comparison justifies the inability of existing techniques in terms of nonlinear data handling functions, data reduction functions and sample retuning functions.

Similarly, Figure 17 depicts the performance comparison of existing systems and proposed OHPAS through PD classification accuracy (%). In this experiment, feature sampling rate (0-1) varies from 0.1 to 1.0 to observe the growing accuracy of PD detection systems.

In this state, feature sampling rate denotes the fulfillment of sampling process during various iterative practices. For example, sampling rate 0.5 indicates the completion of 50% in sampling process. The proficient sampling process generates sufficient number of related samples for increasing the accuracy of classifier. In this regard, the proposed OHPAS produces more significant sample points using VAER practices. Additionally, VAER uses newly generated runtime samples for tuning the LSTM functions to attain better PD detection accuracy rate.

The existing works were limited to nonlinear issues and uncertain data point management. Similarly, the existing systems were not finely implemented for organizing huge dataset contents. In the absence of deeply trained dimensionality reduction procedures, the existing systems produce wide range of samples that are not optimal. Consequently, this affects classifier accuracy rate. Thus the proposed system attains good accuracy than other systems. Consequently, the classification accuracy of proposed OHPAS reaches 99.8% for successful sampling executions. At the same time, CPDS and MVPDS attain 87.5% to 90% of accuracy which are lesser than proposed OHPAS (99.8%). The difference in classification accuracy (10%-12%) is more crucial under real-time PD diagnosis model.

Figure 18 gives the detailed comparisons related to system specificity (%). Specificity shows the system performance on detecting the people those are not having PD symptoms. The existing systems and the proposed system are competing closely during the early stages of sampling but deviated at the end points. The proposed OHPAS maintains 99.8% of specificity at the completion of sampling process. At the same time, other systems produce the specificity rate between 77.1% and 87% at the end. Due to the limitations of dimensionality handling procedures and deep clustering practices, the existing systems lack to attain regulated data features (samples). Thus the existing systems fall under expected performance. In the same manner, Figure 19 delivers system

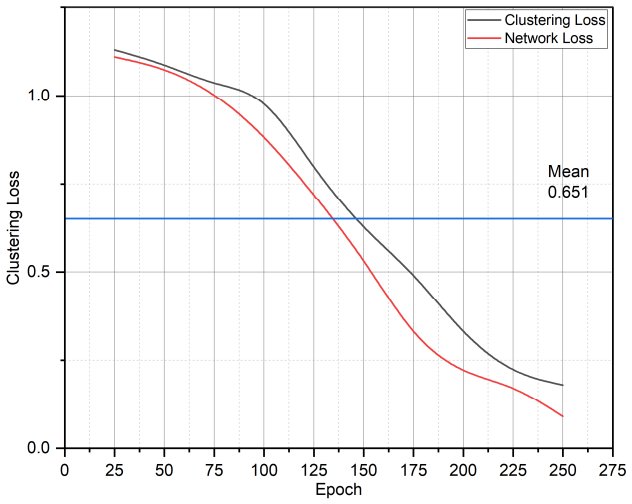

FIGURE 14. Clustering loss and network loss.

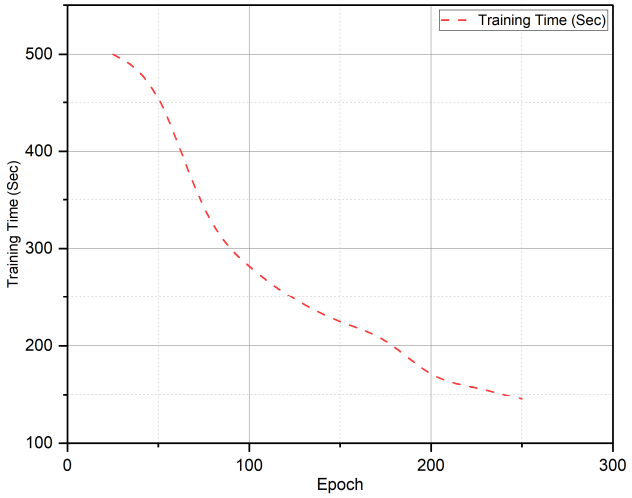

FIGURE 15. Overall system training time.

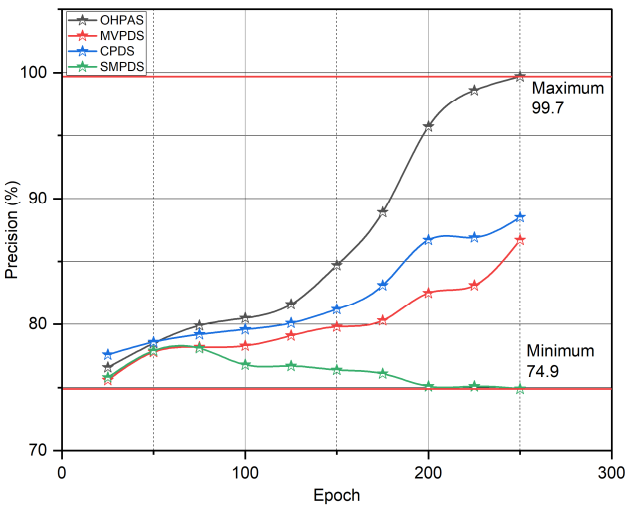

FIGURE 16. System precision.

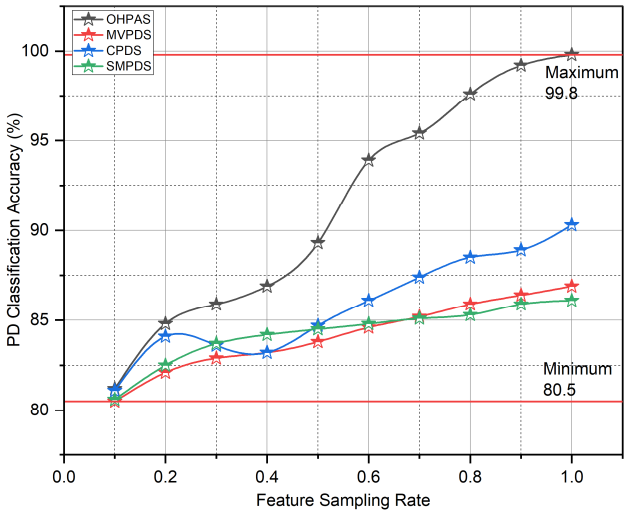

FIGURE 17. Feature classification accuracy.

response time with respect to observation time. Response time is defined as the time taken between sensor data initialization moment and output generation moment. As this proposed system works with real-time body sensor environment, the response time is considered as the crucial factor for providing faster early detection solutions against the symptoms of PD.

As given in Figure 19, the response time of each PD analysis system is observed in milliseconds (msec) over the increasing time durations. The observation periods shall be considered as individual iteration. Each observation period is changing from 15 seconds to 35 seconds depends on the required sensor data points.

In this case, the average response time of existing techniques are varying from 300 msec to 720 msec. The higher response time of existing techniques justifies the overloaded operations of PD symptom analysis techniques over the dataset. Thus the techniques SMPDS, CPDS and MVPDS take more time to create PD response comparing to OHPAS. On contrast, the proposed OHPAS takes only 350 msec of maximum response time. Comparing the response times of various PD detection systems, CPDS uses CNN architectures and OHPAS uses DC (VAER, K-Means, LSTM) architectures for Input/output (IO) management. On the other hand, SMPDS uses RF and SVM units for detecting the symptoms. Nevertheless, SMPDS produces limited accuracy, precision, and specificity rates. The difference between the proposed OHPAS and other systems is not crucial. Though, the proposed OHPAS gives better accuracy than other systems with optimal response time.

The integration of LSTM and VAER predicts the sensor data sequences in a time-series manner. Figure 20 shows the multi-sensor data prediction during the forthcoming days. Notably, this shows the coefficient of variation for each sensor data sequence. In this experiment, the proposed system produces the sensor data predictions for the next 10 days to help the PD patients. This observation assists the patients to

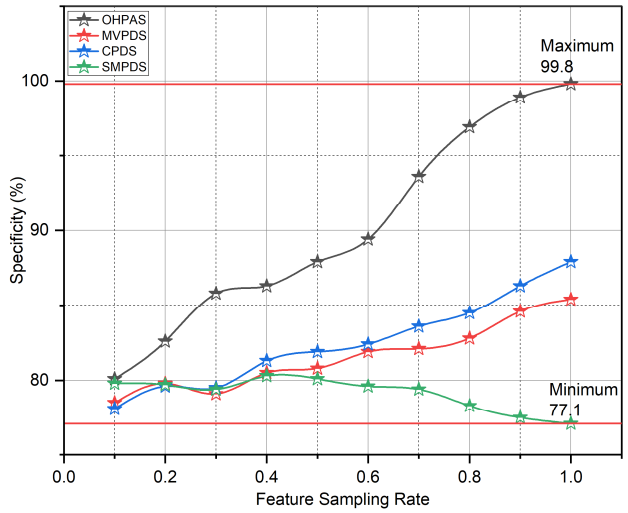

FIGURE 18. System specificity.

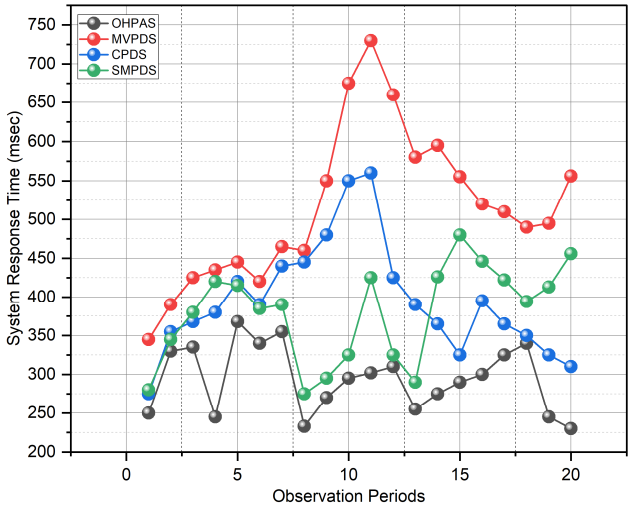

FIGURE 19. System response time.

know the abrupt variants in each body sensor data during recent future times. The coefficient of variation for sensor data prediction shall be defined as given in equation (24).

$$Cv = \frac{d}{m} \tag{24}$$

Equation (24) denotes standard deviation as d and mean value as m.

Similarly, finding system error is the best practice to retune the system performance.

Table 4 gives Root Mean Square Error (RMSE) for existing system and proposed OHPAS. It shows the OHPAS produces 0.03 RMSE under one scale range. Others generate RMSE in the range between 0.18 to 0.23, which affects the system quality in PD detection and prediction tests. The detailed experiment and observations describe the competitive and reactive performance of proposed OHPAS comparing to other existing systems.

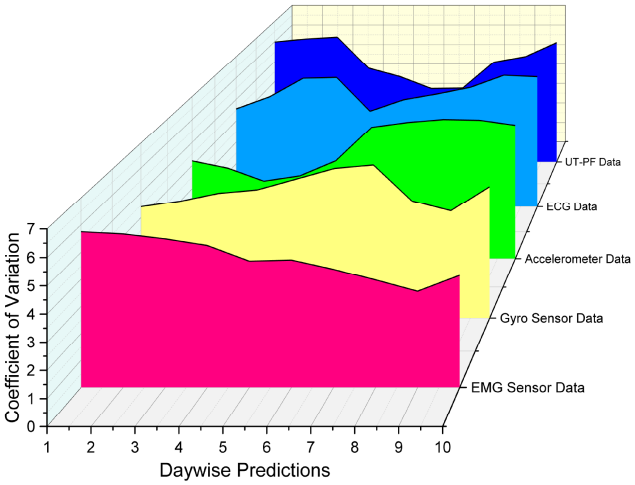

FIGURE 20. Day wise multi-sensor data predictions.

TABLE 4. RMSE.

PD Detection Systems	RMSE Range
OHPAS	0.03
MVPDS	0.18
CPDS	0.14
SMPDS	0.23

TABLE 5. Patient-care experimental solutions.

Patient Identifier	Age	CoV	Duration	PD Stage
1001	45	7.75	16	4
1002	52	6.35	14	4
1003	53	2.34	15	1
1004	38	4.13	13	2
1005	66	4.98	22	3
1006	61	5.52	20	3
1007	73	8.12	17	5
1008	49	8.34	25	5
1009	44	3.35	32	2
1010	40	3.12	29	2

From the deep analysis of PD symptoms using body sensor networks, the improved data prediction quality and treatment quality are assured during the actual practical cases of PD. In this regard, Figure 20 illustrates the prediction sequence of body sensor networks. The forecasted sensor data streams help the patient to get early treatment sessions. At the same time, the doctors can easily observe either severity or degradation of PD stages from the observed sensor data. Table 5 describes the significance of proposed OHPAS against the actual PD cases.

As mentioned in Table 5, the actual testbed examines 10 patients at different ages. Each patient's sensor coefficient

TABLE 6. Affected body portions.

Patient Identifier	Gender	Affected Cases	Acoustic Cases	Time (msec)
1001	Male	Left	Shaky-2	243
1002	Female	Right	Shaky-2	233
1003	Female	Right	Shaky-1	256
1004	Female	Right	Shaky-1	297
1005	Male	Right	Shaky-1	346
1006	Male	Left	Shaky-1	309
1007	Female	Right	Shaky-3	310
1008	Male	Left	Shaky-3	223
1009	Male	Left	Shaky-1	200
1010	Female	Left	Shaky-1	210

of variation (CoV) is the major factor for understanding the current PD severities. In order to monitor the stages of PD symptoms, each patient is monitored with the help of body sensor patches for varying time durations. The monitoring period for each patient vary from 13 days to 32 days according to the observation of optimal CoV. Consequently, the stages are classified by doctor panel.

In this experiment, stage 1 denotes early state of PD symptoms. To prove the essentials of proposed system, Table 6 shows the affected portions and acoustic distortions of each patient. As a continuation of stage-wise observations, the exact affected portions are recognized as either left side movements or right side movements using MC-10 patches. At the same time, MC-1500 and UT-PF sensors are used to observe shaky acoustic cases to ensure the PD symptoms. In this regard, the lower number represents early stage of acoustic shaky conditions.

On the basis of actual medical experiments, we justify the proposed OHPAS optimally detects the symptoms of PD with better accuracy rate at minimal response time. As given in Table 6, the OHPAS response time is varying between 200 msec and 346 msec. The live PDS monitoring and assisting framework has been ensured by the proposed OHPAS comparing to other diagnosis solutions.

V. CONCLUSION

The clinical tests against growing PD need an accurate computer-based diagnosis system to support the patients' life. Under this critical stand, ML and DL-based PD diagnosis solutions help the patients. Recent research works initiated the practices of deep PD symptoms analysis, early PD detection model, body sensor experiments, and artificial diagnosis techniques. However, the existing techniques found difficulty in PD data processing phases, irrelevant data reduction, and effective symptoms monitoring practices. In this regard, the proposed system developed OHPAS for implementing effective symptoms monitoring and patient assisting environment using deeply trained IoT-based body sensor networks. The proposed system enabled multiple body sensor patches that communicate with data processing modules to produce instance responses to the patients. This system planted multiple body sensor patches on human skin. These sensor data sequences were collected and processed with the help of VAER, K-Means clustering, and LSTM techniques to extract the PD symptoms as early as possible. Notably, LSTM-assisted PD analysis model was used to process multi-sensor data streams under live conditions. The proposed technique detected the current PD symptoms and predicted the future symptoms using effective multi-sensor time series analysis models. The deeply trained PD monitoring environment assisted the patients against the symptoms of PD in real-time. The results shown the proposed OHPAS performed significantly than other existing systems. However, this proposed work has platform-level difficulties and product-level limitations. The hardware components and deployment difficulties should be improved in the future.

REFERENCES

[1] Z. Soumaya, B. D. Taoufiq, N. Benayad, K. Yunus, and A. Abdelkrim, "The detection of Parkinson disease using the genetic algorithm and SVM classifier," *Appl. Acoust.*, vol. 171, Jan. 2021, Art. no. 107528.

[2] J. Jankovic and E. Anthony, "Diagnosis and assessment of Parkinson disease and other movement disorders," in *Bradley's Neurology in Clinical Practice E-Book*, vol. 310, no. 1. U.K.: Elsevier, 2021.

[3] J. Galper, M. Balwani, S. Fahn, C. Waters, L. Krohn, Z. Gan-Or, N. Dzamko, and R. N. Alcalay, "Cytokines and Gaucher biomarkers in glucocerebrosidase carriers with and without Parkinson disease," *Movement Disorders*, vol. 36, no. 6, pp. 1451–1455, Jun. 2021.

[4] M. Son, S. H. Han, C. H. Lyoo, J. A. Lim, J. Jeon, K.-B. Hong, and H. Park, "The effect of levodopa on bilateral coordination and gait asymmetry in Parkinson's disease using inertial sensor," *npj Parkinson's Disease*, vol. 7, no. 1, pp. 1–7, Dec. 2021.

[5] J. H. Park, C. Lee, M. J. Nam, H. Kim, D. Y. Kwon, J. W. Yoo, and L. Kyu, "Association of high-density lipoprotein cholesterol variability and the risk of developing Parkinson disease," *Neurology*, vol. 96, no. 10, pp. 1391–1401, 2021.

[6] S. Bind, T. Arvind, S. Anil, P. M. Koulibaly, F. Nobili, M. Pagani, O. Sabri, T. V. Borght, K. V. Laere, and K. Tatsch, "A survey of machine learning based approaches for Parkinson disease prediction," *Int. J. Comput. Sci. Inf. Technol.*, vol. 6, no. 2, pp. 1648–1655, 2015.

[7] O. Yaman, F. Ertam, and T. Tuncer, "Automated Parkinson's disease recognition based on statistical pooling method using acoustic features," *Med. Hypotheses*, vol. 135, Feb. 2020, Art. no. 109483.

[8] V. Mittal and R. K. Sharma, "Machine learning approach for classification of Parkinson disease using acoustic features," *J. Reliable Intell. Environments*, vol. 7, no. 3, pp. 233–239, Sep. 2021.

[9] K. Polat and M. Nour, "Parkinson disease classification using one against all based data sampling with the acoustic features from the speech signals," *Med. Hypotheses*, vol. 140, Jul. 2020, Art. no. 109678.

[10] R. F. Pfeiffer, "Non-motor symptoms in Parkinson's disease," *Parkinsonism Rel. Disorders*, vol. 22, no. 1, pp. 22–119, 2016.

[11] A. H. V. Schapira, K. R. Chaudhuri, and P. Jenner, "Non-motor features of Parkinson disease," *Nature Rev. Neurosci.*, vol. 18, no. 7, pp. 435–450, Jul. 2017.

[12] F. Ba, M. Obaid, M. Wieler, R. Camicioli, and W. R. W. Martin, "Parkinson disease: The relationship between non-motor symptoms and motor phenotype," *Can. J. Neurolog. Sci.* , vol. 43, no. 2, pp. 261–267, Mar. 2016.

[13] S. Grover, S. Bhartia, A. Yadav, and K. R. Seeja, "Predicting severity of Parkinson's disease using deep learning," *Proc. Comput. Sci.*, vol. 132, no. 1, pp. 1788–1794, May 2018.

[14] S. Sivaranjini and C. M. Sujatha, "Deep learning based diagnosis of Parkinson's disease using convolutional neural network," *Multimedia Tools Appl.*, vol. 79, nos. 21–22, pp. 15467–15479, 2020.

[15] M. Kahya, K. E. Lyons, R. Pahwa, A. E. Akinwuntan, J. He, and H. Devos, "Reliability and validity of pupillary response during dual-task balance in Parkinson disease," *Arch. Phys. Med. Rehabil.*, vol. 102, no. 3, pp. 448–455, Mar. 2021.

[16] C. Flagg, O. Frieder, S. MacAvaney, and G. Motamedi, "Real-time streaming of gait assessment for Parkinson's disease," in *Proc. 14th ACM Int. Conf. Web Search Data Mining*, Mar. 2021, vol. 1, no. 1, pp. 1081–1084.

[17] A. Polo-Morales, Á. Alcocer-Salas, M. Rodríguez-Violante, D. Pinto-Solís, R. Solís-Vivanco, and A. Cervantes-Arriaga, "Association between somatization and nonmotor symptoms severity in people with Parkinson disease," *J. Geriatric Psychiatry Neurol.*, vol. 34, no. 1, pp. 60–65, Jan. 2021.

[18] K. Chen, D. Zhang, L. Yao, B. Guo, Z. Yu, and Y. Liu, "Deep learning for sensor-based human activity recognition: Overview, challenges, and opportunities," *ACM Comput. Surv.*, vol. 54, no. 4, pp. 1–40, May 2022.

[19] G. Nagasubramanian and M. Sankayya, "Multi-variate vocal data analysis for detection of Parkinson disease using deep learning," *Neural Comput. Appl.*, vol. 33, no. 10, pp. 4849–4864, May 2021.

[20] E. Balaji, D. Brindha, and R. Balakrishnan, "Supervised machine learning based gait classification system for early detection and stage classification of Parkinson's disease," *Appl. Soft Comput.*, vol. 94, no. 1, Sep. 2020, Art. no. 106494.

[21] M. Diaz, M. Moetesum, I. Siddiqi, and G. Vessio, "Sequence-based dynamic handwriting analysis for Parkinson's disease detection with one-dimensional convolutions and BiGRUs," *Expert Syst. Appl.*, vol. 168, Apr. 2021, Art. no. 114405.

[22] R. Powers, M. Etezadi-Amoli, E. M. Arnold, S. Kianian, I. Mance, M. Gibiansky, D. Trietsch, A. S. Alvarado, J. D. Kretlow, T. M. Herrington, S. Brillman, N. Huang, P. T. Lin, H. A. Pham, and A. V. Ullal, "Smartwatch inertial sensors continuously monitor real-world motor fluctuations in Parkinson's disease," *Sci. Transl. Med.*, vol. 13, no. 579, p. 7865, Feb. 2021.

[23] A. Mirelman *et al.*, "Detecting sensitive mobility features for Parkinson's disease stages via machine learning," *Movement Disorders*, vol. 36, no. 9, pp. 2144–2155, Sep. 2021.

[24] D. J. Park, J. W. Lee, M. J. Lee, S. J. Ahn, J. Kim, G. L. Kim, Y. J. Ra, Y. N. Cho, and W. B. Jeong, "Evaluation for parkinsonian bradykinesia by deep learning modeling of kinematic parameters," *J. Neural Transmiss.*, vol. 128, no. 2, pp. 181–189, Feb. 2021.

[25] A. S. Ashour, A. El-Attar, and N. Dey, "Long short term memory based patient-dependent model for FOG detection in Parkinson's disease," *Pattern Recognit. Lett.*, vol. 131, pp. 23–29, Mar. 2020.

[26] A. Naseer, M. Rani, S. Naz, M. I. Razzak, M. Imran, and G. Xu, "Refining Parkinson's neurological disorder identification through deep transfer learning," *Neural Comput. Appl.*, vol. 32, no. 3, pp. 839–854, Feb. 2020.

[27] H. Ali Hashim, S. L. Mohammed, and S. K. Gharghan, "Accurate fall detection for patients with Parkinson's disease based on a data event algorithm and wireless sensor nodes," *Measurement*, vol. 156, May 2020, Art. no. 107573.

[28] S. Pardoel, J. Kofman, J. Nantel, and E. D. Lemaire, "Wearable-sensor-based detection and prediction of freezing of gait in Parkinson's disease: A review," *Sensors*, vol. 19, no. 23, p. 5141, Nov. 2019.

[29] L. Lonini, A. Dai, N. Shawen, T. Simuni, C. Poon, L. Shimanovich, M. Daeschler, R. Ghaffari, J. A. Rogers, and A. Jayaraman, "Wearable sensors for Parkinson's disease: Which data are worth collecting for training symptom detection models," *npj Digit. Med.*, vol. 1, no. 1, pp. 1–8, Dec. 2018.

[30] S. Aich, M. P. Pyari, C. Sabyasachi, K. Hee, K. Hee, L. Hae, K. Hwan, J. Moon, J. S. Sim, and P. Jinse, "Design of a machine learning-assisted wearable accelerometer-based automated system for studying the effect of dopaminergic medicine on gait characteristics of Parkinson's patients," *J. Healthcare Eng.*, vol. 1, no. 1, 2020, Art. no. 1823268.

[31] K. Kyritsis, P. Fagerberg, I. Ioakimidis, K. R. Chaudhuri, H. Reichmann, L. Klingelhoefer, and A. Delopoulos, "Assessment of real life eating difficulties in Parkinson's disease patients by measuring plate to mouth movement elongation with inertial sensors," *Sci. Rep.*, vol. 11, no. 1, pp. 1–14, Dec. 2021.

[32] J. F. Daneault, V. D. Gloria, P. Federico, A. Chen, A. Christina, B. Matilde, and B. Edoardo, "Accelerometer data collected with a minimum set of wearable sensors from subjects with Parkinson's disease," *Sci. Data*, vol. 8, no. 1, pp. 1–13, Dec. 2021.

[33] O. Karaman, H. Çakın, A. Alhudhaif, and K. Polat, "Robust automated Parkinson disease detection based on voice signals with transfer learning," *Expert Syst. Appl.*, vol. 178, no. 1, Sep. 2021, Art. no. 115013.

[34] M. Zhong, L. Zhang, X. Liu, Y. Zhou, M. Zhang, Y. Wang, L. Yang, and D. Wei, "Wide linear range and highly sensitive flexible pressure sensor based on multistage sensing process for health monitoring and human-machine interfaces," *Chem. Eng. J.*, vol. 412, no. 1, May 2021, Art. no. 128649.

[35] A. Marcante, R. Di Marco, G. Gentile, C. Pellicano, F. Assogna, F. E. Pontieri, G. Spalletta, L. Macchiusi, D. Gatsios, A. Giannakis, M. Chondrogiorgi, S. Konitsiotis, D. I. Fotiadis, and A. Antonini, "Foot pressure wearable sensors for freezing of gait detection in Parkinson's disease," *Sensors*, vol. 21, no. 1, p. 128, Dec. 2020.

[36] M. Sica, T. Salvatore, C. Colum, K. Lorna, M. Kevin, T. Suzanne, B. John, O. Brendan, and K. Dimitrios, "Continuous home monitoring of Parkinson's disease using inertial sensors: A systematic review," *PLoS ONE*, vol. 16, no. 2, 2021, Art. no. 246528.

[37] C. Agurto, S. Heisig, A. Abrami, B. K. Ho, and V. Caggiano, "Parkinson's disease medication state and severity assessment based on coordination during walking," *PLoS ONE*, vol. 16, no. 2, 2021, Art. no. 244842.

[38] A. Rodríguez-Molinero, P. Carlos, S. Albert, M. Eva, R. Daniel, H. Jorge, and B. Àngels, "A kinematic sensor and algorithm to detect motor fluctuations in Parkinson disease: Validation study under real conditions of use," *JMIR Rehabil. Assistive Technol.*, vol. 5, no. 1, p. 8335, 2018.

[39] B. Lieber, B. E. S. Taylor, G. Appelboom, G. McKhann, and E. S. Connolly, "Motion sensors to assess and monitor medical and surgical management of Parkinson disease," *World Neurosurg.*, vol. 84, no. 2, pp. 561–566, Aug. 2015.

[40] F. Rahimi, C. Duval, M. Jog, C. Bee, A. South, M. Jog, R. Edwards, and P. Boissy, "Capturing whole-body mobility of patients with Parkinson disease using inertial motion sensors: Expected challenges and rewards," in *Proc. Annu. Int. Conf. IEEE Eng. Med. Biol. Soc.*, Aug. 2011, vol. 1, no. 1, pp. 5833–5838.

[41] M. Jauhiainen, P. Juha, M. Saeed, R. Jari, H. Anu, V. Antti, and N. Hannu, "Identification of motor symptoms related to Parkinson disease using motion-tracking sensors at home (KÄVELI): Protocol for an observational case-control study," *JMIR Res. Protocols*, vol. 8, no. 3, p. 12808, 2019.

[42] R. Bhidayasiri, J. Sringean, P. Taechalertpaisarn, and C. Thanawattano, "Capturing nighttime symptoms in Parkinson disease: Technical development and experimental verification of inertial sensors for nocturnal hypokinesia," *J. Rehabil. Res. Develop.*, vol. 53, no. 4, pp. 487–498, 2016.

[43] S. Sawilowsky and G. Fahoome, "Kruskal-Wallis Test: Basic," in *Wiley StatsRef: Statistics Reference Online*, vol. 1. Hoboken, NJ, USA: Wiley, 2014.

[44] W. Yin, K. Kann, M. Yu, and H. Schütze, "Comparative study of CNN and RNN for natural language processing," 2017, *arXiv:1702.01923*.

[45] T. van Erven and P. Harremos, "Rényi divergence and Kullback–Leibler divergence," *IEEE Trans. Inf. Theory*, vol. 60, no. 7, pp. 3797–3820, Jul. 2014.

[46] A. G. Malek, M. Mansoori, and H. Omranpour, "Random forest and rotation forest ensemble methods for classification of epileptic EEG signals based on improved 1D-LBP feature extraction," *Int. J. Imag. Syst. Technol.*, vol. 31, no. 1, pp. 189–203, Mar. 2021.

[47] M. A. Khan, S. A. Memon, F. Farooq, M. F. Javed, F. Aslam, and R. Alyousef, "Compressive strength of fly-ash-based geopolymer concrete by gene expression programming and random forest," *Adv. Civil Eng.*, vol. 2021, pp. 1–17, Jan. 2021.

[48] S. Chandra, A. Chandra, and R. Gupta, "An efficient data routing scheme for multi-patient monitoring in a biomedical sensor network through energy equalization strategy," *Wireless Netw.*, vol. 27, no. 1, pp. 635–648, Jan. 2021.

[49] N. Rohaizad, C. C. Mayorga-Martinez, M. Fojtå, N. M. Latiff, and M. Pumera, "Two-dimensional materials in biomedical, biosensing and sensing applications," *Chem. Soc. Rev.*, vol. 50, no. 1, pp. 619–657, 2021.

[50] N. L. Kazanskiy, S. N. Khonina, M. A. Butt, A. Kaźmierczak, and R. Piramidowicz, "State-of-the-art optical devices for biomedical sensing applications—A review," *Electronics*, vol. 10, no. 8, p. 973, Apr. 2021.

[51] T. Yokota, K. Fukuda, and T. Someya, "Recent progress of flexible image sensors for biomedical applications," *Adv. Mater.*, vol. 33, no. 19, May 2021, Art. no. 2004416.

[52] S. Rajasoundaran, A. V. Prabu, G. S. Kumar, P. P. Malla, and S. Routray, "Secure opportunistic watchdog production in wireless sensor networks: A review," *Wireless Pers. Commun.*, vol. 120, no. 2, pp. 1895–1919, Sep. 2021.

[53] C. Girerd, Q. Zhang, A. Gupta, M. Dunna, D. Bharadia, and T. K. Morimoto, "Towards a wireless force sensor based on wave backscattering for medical applications," *IEEE Sensors J.*, vol. 21, no. 7, pp. 8903–8915, Apr. 2021.
[54] D. Formica and E. Schena, "Smart sensors for healthcare and medical applications," *Sensors*, vol. 21, no. 2, p. 543, Jan. 2021.

RAJASOUNDARAN SOUNDARARAJAN is currently an Assistant Professor with the School of Computer Science and Engineering, VIT University, Bhopal, Madhya Pradesh, India.

A. V. PRABU is currently an Associate Professor in electronics and communication engineering with the Koneru Lakshmaiah Education Foundation (Deemed to be University), Vaddeswaram, Andhra Pradesh, India.

SIDHESWAR ROUTRAY received the B.Tech. and M.Tech. degrees from the Biju Patnaik University of Technology, Rourkela, Odisha, India, in 2009 and 2012, respectively.

PRINCE PRIYA MALLA received the B.Tech. and M.Tech. degrees in electronics and communication engineering from the Biju Patnaik University of Technology, Rourkela, Odisha, India, in 2010 and 2012, respectively.

ARUN KUMAR RAY received the Ph.D. degree from IIT Kharagpur. He is currently working as a Professor with the School of Electronics Engineering, and KIIT Deemed to be University. He is acting as the Director Academics of the university. He is now involved both in teaching and administration.

GOPINATH PALAI is currently working as a Professor with the Department of Electronics and Communication Engineering, Gandhi Institute of Technological Advancements, Bhubaneswar, India.

OSAMA S. FARAGALLAH is currently a Professor with the Department of Information Technology, College of Computers and Information Technology, Taif University, Saudi Arabia.

MOHAMMED BAZ (Senior Member, IEEE) is currently an Associate Professor at the Department of Computer Engineering, College of Computers and Information Technology, Taif University, Taif, Saudi Arabia.

MATOKAH M. ABUALNAJA is currently an Associate Professor at the Department of Chemistry, Faculty of Applied Science, Umm Al-Qura University, Mecca, Saudi Arabia.

MOHAMOUD M. A. EID is currently an Assistant Professor with the Electrical Engineering Department, Faculty of Engineering, Taif University.

AHMED NABIH ZAKI RASHED is currently with the Faculty of Electronic Engineering, Menoufia University, Egypt. He has published more than 349 articles in high impacted journals and an editor in many international journals. He was selected among the top 2% of scientists published by Stanford University.